RESEARCH

Check for updates

Insight on molecular interactions in shrinkage of Na-montmorillonite clay by molecular dynamics simulation

**Wei-Qiang Feng · Kamal Al-Zaoari ·
Ze-Jian Chen**

Abstract Expansive soils are known to be hazardous materials for infrastructure due to their high shrinking or swelling potential. Understanding the shrinking factors of expansive soils such as montmorillonite (MMT) is essential for predicting their mechanical properties. The interactions between the components of Na-MMT clays, e.g., MMT layer–layer (LL), layer–cation (LC), layer–water (LW) and water–cation (WC), are responsible for its shrinking behavior. In this study, molecular dynamics simulation and grand canonical Monte Carlo simulations are used to investigate the interaction energy evolution in the layered structure of Na-MMT for the shrinkage mechanisms analysis of clay. The results of simulation indicate that the magnitude of the interaction energy contributed by the interlayer cations dehydration is the driving force of the interlayer shrinkage. Furthermore, in the hydrated state, with one water layer, two water layers and three water layers, the attractive interactions between WC and LW, maintain the stability of the clay layers. However, at the dry state, the interaction energy between layers and cations appears to be the most essential component in holding the stacked layers together, which provides structural stability to the clay sheets. Finally, the study reveals that intermolecular interactions contribute to the mechanical properties of clays such as cohesive and elastic properties.

Keywords Molecular dynamics simulation · Interaction energy · Shrinkage behavior · Cation dehydration

1 Introduction

Smectites are ubiquitous clay minerals in the earth surface environments, where the minerals display a wide range of crystal–chemistry properties. Smectite clays are observed to swell significantly when exposed to water, and shrink as the water drains (Fu et al. 1990). The swelling-shrinkage behavior of smectite clays is the basic factor of many geotechnical and geo-environmental engineering challenges (Amarasinghe and Anandarajah 2012; Acharya et al. 2015; Anandarajah and Amarasinghe 2013; Song et al. 2024). The swelling–shrinkage rotation may produce a great deal of stress, which might damage a variety of engineering structures (Wang and Wei 2015; Acharya et al. 2015; Anandarajah and

W.-Q. Feng · K. Al-Zaoari
Department of Ocean Science and Engineering, Southern University of Science and Technology, Shenzhen, China
e-mail: fengwq@sustech.edu.cn

K. Al-Zaoari
e-mail: 12231430@mail.sustech.edu.cn

Z.-J. Chen (✉)
Department of Civil and Environmental Engineering, The Hong Kong Polytechnic University, Hong Kong SAR, China
e-mail: zejchen@polyu.edu.hk

Amarasinghe 2013), as shown in Fig. 1. With regard to the multi-scale responses from micro- to atomistic-scale of the soil, understanding the swelling-shrinkage process of smectite is crucial for predicting soil behavior in the short- and long-term requirements.

As montmorillonite (MMT) is the principal component of smectites, which plays a vital role in the swelling and shrinking behaviors of expansive soils, it has been studied extensively by experimental and numerical methods (Amarasinghe and Anandarajah 2013; Boek 2014; Boek et al.1995; Bowers et al. 2011; Katti et al. 2018; Li et al. 2024; Norrish 1954; Tajeddine et al. 2015; Villar et al. 2012; Zheng and Zaoui 2013; Vydelingum et al. 2023). Norrish (1954) used X-ray diffraction to study the swelling of montmorillonite in salt solutions and found that the type of interlayer cations and their hydration energy affect the initial swelling. Fu et al. (1990) found that the clay structure varies during the swelling-shrinking cycle and is governed by the relative humidity and bending of the adsorbed water, as well as the level of interaction between the clay layers. Michot et al. (2005) investigated the effect of layer charge on the swelling-shrinkage process. The result demonstrated that cohesiveness between layers rises with increasing layer charge, and highly charged clay layers are difficult to swell in the early swelling state. He et al. (2020) conducted an experimental investigation to study the effects of salt solution on the swelling and shrinkage behavior of expansive soils and found that the swelling strain of bentonite decreases from 177% in pure water to 75% in NaCl solution. Henok et al.

(2021) presented that the swelling-shrinking behavior of the examined soils is closely related to temperature: the higher the temperature, the larger the shrinkage. These results show that thermal and saline environments have a significant impact on the swelling-shrinkage behavior of MMT soils.

Besides experimental techniques, molecular simulations are complementary techniques for studying the complex structure and interlayer interactions in montmorillonite. Molecular simulations can provide a more detailed picture of the interlayer structure evolution, the interlayer water and cations transition, and their thermodynamic properties (Al-Zaoari et al. 2022; Chen et al. 2023; Cygan et al. 2021), which are challenging to accurately measure in experiments. For the simulation of swelling-shrinkage in clay mineral systems, there are two major methods: molecular dynamics (MD) and Monte Carlo (MC), which are based on dynamics and classical statistical mechanics, respectively (Anderson et al. 2010). Yotsuji et al. (2021) examined the crystalline swelling of MMT with diverse interlayer cations with experimental measurements and MD simulations and found a good agreement between MD simulation and experimental results in terms of swelling mechanism and interlayer cation influence. MD and discrete-element method (DEM) simulations were used to study the swelling mechanism of MMT, and it was found that the interlayer forces, as well as the interlayer ions species, play a key role in the crystalline expansion (Amarasinghe and Anandarajah 2013; Anandarajah and Amarasinghe 2013). Other MD simulations
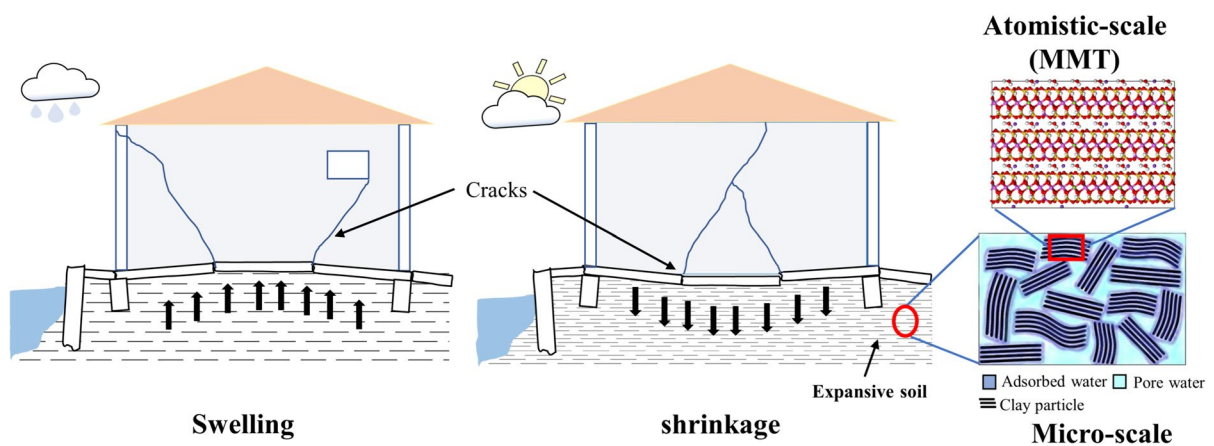

Fig. 1 Schematic diagram of expansive soil hazards to engineering structures and an illustration of various scales of swelling clay

focused on the structure and dynamic features of the hydrated MMT, calculation of the diffusion coefficient of water molecules and interlayer cations, as well as the basal spacing (Chang 1995; Marry 2002; Norrish 1954; Zhang 2016; Zheng and Zaoui 2011; Liu 2021), which showed that the hydration swelling of MMT is influenced by interlayer cation and internal surface charge (Young and Smith 2000). Wei et al. (2022) investigated the sensitivity of water content and structural anisotropy on the mechanical behavior of MMT with the help of hydrogen bonds in MD simulations. The Monte Carlo approach was used to simulate the hydration swelling of Li-MMT, Na-MMT, and K-MMT, revealing that sodium and lithium are considerably easier to hydrate than potassium (Boek et al. 1995).

Molecular interactions in the interlayer of MMT are responsible for clay strength, durability, and thermal properties. With varying amounts of water adsorbed or desorbed in the interlayer of clays, the interlayer spacing is determined by the equilibrium of nonbonded interactions between clay layers, water molecules, and cations at a constant temperature and pressure (Li 2020; Pradhan 2015; Ewis et al. 2022; Liu et al. 2022; Dai et al. 2023; Ghazanfari et al. 2023). A detailed understanding of microscale swelling-shrinkage as well as particle layer and interlayer species interactions is demanded. Smith et al. (2006) carried out MC and GCMC simulations on the thermodynamics of clay swelling, in which the temperature- and pressure-dependence of clay swelling was related to the entropy and volume change of the system, and evaluated the chemical potential to determine the basal spacing and adsorption isotherms. Abduljauwad et al. (2017) investigated the swelling potential of MMT from the perspective of cohesive energy density. Katti et al. (2018) carried out Fourier transform infrared (FTIR) and molecular dynamics simulation to study the swelling behavior of Na-MMT in different organic fluids and found that nonbonded interactions between clay and water are more obvious, indicating that the polarity of fluids plays a significant role in the interlayer swelling-shrinkage. However, most of current studies focus on the interpretation of MMT swelling, but neglect the shrinkage behavior of MMT, especially on the evaluation of interaction energies as well as the effect of temperature and fluid salinity. This limitation may result in some incorrect evaluations of shrinkage behavior in many engineering fields, such as construction, coastal conservation, road paving, etc. Thus, it demands a detailed understanding of microscale shrinkage as well as particle layer and interlayer species interactions.

In this study, we purpose to reveal the different interactions of MMT components during shrinkage (including interaction of layer to layer (LL), interaction of layer to water molecules (LW), interaction of layer to cations (LC), and interaction of water molecules to cations (WC)), and to find the relationship between the shrinkage process and the interlayer change from the perspective of internal interactions. To better understand the impact of temperature and salinity on the mechanical properties of clays during shrinkage, two types of solutions (pure water and NaCl solution) are adopted to represent non-saline and saline environments and three temperatures (273 K, 298 K and 324 K) are considered to simulate the deep-sea, the room, and the high-temperature environments respectively in the MD simulations.

2 Molecular dynamics simulation and procedures

2.1 Model construction

All Molecular Dynamics (MD) and Grand canonical Monte Carlo (GCMC) simulations are performed using Lammps software (Plimpton 1995) and VMD (Humphrey et al. 1996) for visualization and the calculation of the hydrogen bonds. The chemical formula of the MMT models is given as $Na_{0.75}(Al_{3.5}Mg_{0.5}) [Si_{7.75} Al_{0.25}] O_{20}(OH_4)$ (Boek et al. 1995). The atomic coordinates of the unit cell are $a = 5.175$ Å, $b = 8.896$ Å. The MMT model consists of two layers ($4a \times 2b \times 2c$) with 195 water molecules, which are continuous in three directions through the periodic boundary. These layers are negatively charged because of the substitution of Mg^{2+} for Al^{3+} in the octahedral sheets and that of Al^{3+} for Si^{4+} in the tetrahedral sheets (Du et al. 2022). This substitution creates a negative layer charge of -0.75 e/uc which is balanced by the interlayer cations (0.75 Na/uc). For saline environment simulation, NaCl is added in the interlayer, assuming that salt ions diffuse into the interlayer of MM, with a salt concentration of about 34 g/kg, which is close to the salt concentration of seawater (Birgersson and Karnland 2009; Camara
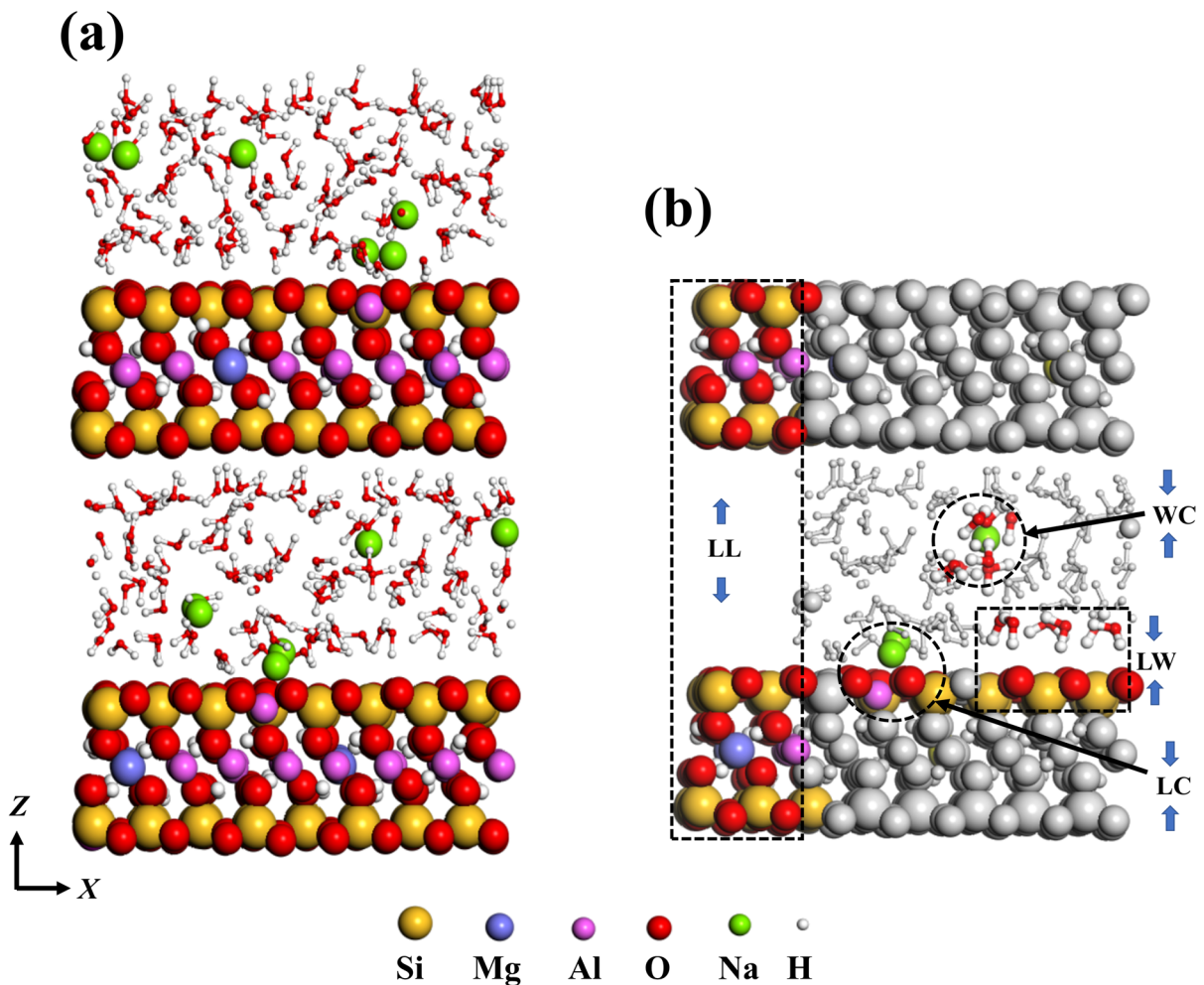
Fig. 2 Schematic representation of MMT model and four categories of MMT interactions: **a** MMT initial model; **b** diagram of four categories of MMT interactions: layer–layer (LL), layer–cation (LC), layer–water (LW) and water–cation (WC)

et al. 2017; Aoyama et al. 2002). A representative schematic diagram of the Na-montmorillonite model and categories of MMT interactions are shown in Fig. 2.

2.2 Simulation details

The Na-MMT model is initialized with cations located in the midplane of the interlayer and water molecules inserted above and below the cations. Independent MD simulations are first performed for thermodynamic equilibrium. The energy minimization and geometry optimization are performed, and random interlayer configurations are generated in the canonical (NVT) ensemble for 50 ps with a time step of 1.0 fs, where all atoms are allowed to move, followed by a further equilibration in the isothermal-isobaric (NPT) ensemble lasting 500 ps until the system achieves its equilibrium state. Next, the model is brought to a shrinking process by GCMC and MD simulations.

GCMD simulation has been applied to study the adsorption and desorption properties of water in absorbent materials as it is a flexible and effective technique (Botan et al. 2011). Since the temperature, volume, and number of atoms in MD are fixed, the GCMC is a

better choice to simulate an open system, in which the temperature, volume, and chemical potential are fixed while the number of atoms and molecules in the system is allowed to vary. Therefore, a cycle of GCMC and MD is used in this study to simulate the desorption of water. For each cycle, the GCMC which consists of N Monte Carlo attempts and (NMC) of particle insertion or deletion, is followed by 2×10^4 MD steps in the NPT ensemble. The chemical potential of the water is defined as the chemical potential (pressure) of the ideal gas reservoir with a value of 1 atm. Only water molecules are allowed to move (delete) in the GCMC and the MD allows the system to equilibrate after the change of water molecules in the system. Thus, the shrinking of MMT is generated by the GCMC deletion of water molecular and MD equilibrium processes. Over the last step of MD runs, every 20 ps, the configurations of the system are recorded for further energy and structural analysis. The MD simulations last for 900 ps before MMT dries out.

In the MD simulation, the temperature of 273 K, 289 K, 324 K and the pressure of 1 atm are controlled by Nosé-Hoover thermostat and barostat, respectively. The coupling constants for the thermostat and barostat are 100- and 1000-time steps, respectively. The Clayff force field is used to describe the interactions between atoms (Cygan et al. 2004). The flexible simple point-charge SPC water model (Berendsen et al. 1981) is used in combination with Clayff. Clayff is dominated by nonbonded interactions (van der Waals and Coulombic), with just layer hydroxyl groups and water molecules exhibiting bonded interactions. The Coulombic interactions are calculated using the Ewald summation, with a cut-off distance of 10 Å, while the Lennard–Jones is used to evaluate the van der Waals interaction:

$$E(r_{ij}) = 4\varepsilon_{ij} \left[\left(\frac{\sigma_{ij}}{r_{ij}} \right)^{12} - \left(\frac{\sigma_{ij}}{r_{ij}} \right)^6 \right] + \frac{q_i q_j}{4\pi\varepsilon_o r_{ij}} \qquad (1)$$

where E is the total potential, r_{ij} is the separation distance, ε_0 is the vacuum dielectric constant, q_i and q_j are the partial charge of atoms i and j, respectively. ε_{ij} is the Lennard–Jones size, σ_{ij} is the Lennard–Jones well depth, see Fig. 3, which can be defined by the following Lorentz-Berthelot combing rule:

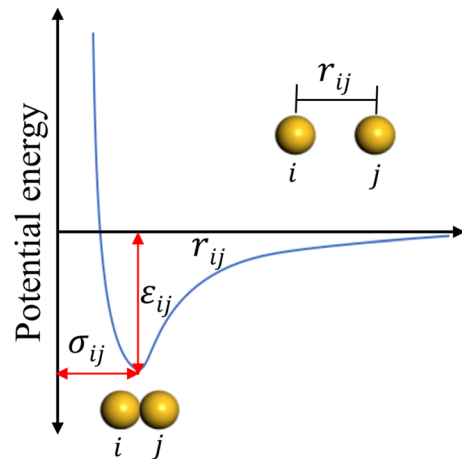$$\varepsilon_{ij} = \sqrt{\varepsilon_i \varepsilon_j} \qquad (2)$$

Fig. 3 Schematic of Lennard–Jones potential between two pairs

$$\sigma_{ij} = \frac{1}{2} \left(\sigma_i + \sigma_j \right) \qquad (3)$$

To calculate the interaction energies of MMT components, groups for the different components (layers, cations, and water molecules) are defined first, and then the pairwise interaction energies between these specified groups are calculated. The interaction energy, which includes both van der Waals and Coulombic interactions, is calculated between all the atoms in the first group and all the atoms in the second group. For instance, to calculate Coulombic interactions, the double sum in Ewald summation is restricted to include only atoms in specific groups A and B, where the term x(k) can be defined as a double sum over particle positions as:

$$x(k) = \sum_{i=1}^{NA} q_i^{e^{ik.ri}} \sum_{j=1}^{NB} q_j^{e^{-jk.rj}} = S_A(k) S_B(-k) \qquad (4)$$

where q_i, q_j are the charge of atoms i and j in group A and B, respectively, r_i, r_j The position vector of atom i and j, k is A reciprocal lattice vector, $S_A(k)$ and $S_B(k)$ are the structure factors for groups A and B, respectively.

3 Results and discussions

MMT shrinkage is defined as a reduction process in the distance between clay layers (basal spacing) as a result of interlayer water molecular desorption. Figure 4a show the number of water molecules at the end of each GCMC cycle. One to four water molecules were deleted in each GCMC attempt, leading to a gradual decrease in the interlayer water content with time. This desorption process was observed to significantly impact the interlayer spacing, contributing to the overall shrinkage of the Na-MMT structure. The linear desorption trend is similar to the adsorption behavior of water molecules into the interlayer spaces of Na-MMT as reported by Svoboda et al. (2018). To confirm the simulation accuracy in this study, the basal spacing of freshwater simulation at 298 K is presented as a function of water content in Fig. 4, and compared to experimental and simulation results in the literature (Fu et al. 1990; Zhang et al. 2011), which indicates the shrinking of Na-MMT through three water layers. The simulation results in this study are found in good agreement with the previous experiment and simulation data.

Furthermore, previous research indicates that Na-MMT exhibits two stable states corresponding to two or three water layers in the crystalline swelling regime (Loganathan et al. 2016; Zhang et al. 2014). However, adding more water beyond these states, the montmorillonite expands continuously without reaching a stable multilayered water configuration. At this stage, the clay layers have expanded sufficiently so that the interlayer water effectively shields the electrostatic interactions (LL). Essentially, at more than three water layers, the system's energy is dominated by the hydrogen bonding among the interlayer water molecules, making the interlayer region behave more like bulk water than structured interlayer water (Cygan et al. 2004).

The change of basal spacing of Na-MMT during the shrinkage with various temperatures and water environments is collected and shown in Fig. 5. The basal spacing curve illustrates the shrinkage manner of Na-MMT as interlayer water content decreases from 0.3 to 0 gW/gC (30 to 0%) with 3 to 0 water layers (3W, 2W, 1W, and 0W). It is observed that, at hydrated state (3W, 2W and 1W), the temperature effect on the basal spacing is minor, especially at low water content, and this agrees with the previous study (Zhang et al. 2010; Teich-McGoldrick et al. 2015). Nevertheless, at dry state, temperature has remarkable influences on the basal spacing in salt water simulation. It is found that the basal spacing under 298 K is smaller than that under 273 K while the basal
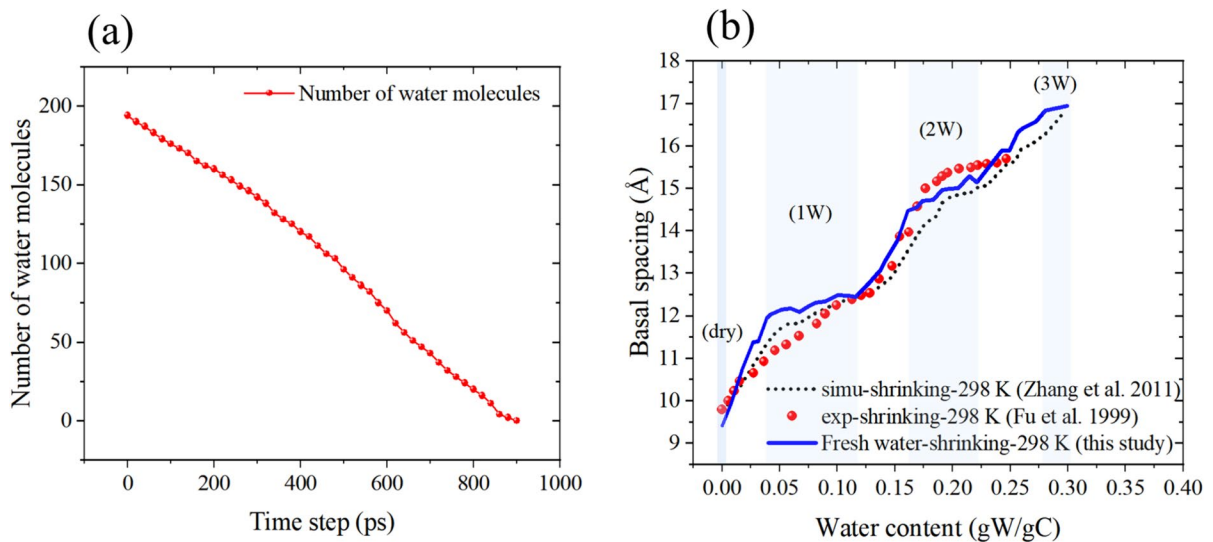

Fig. 4 **a** The number of water molecules with time step during GCMC cycles at 298 K. **b** The basal spacing of Na-MMT in this work at 298 K compared with previous simulation and experiment results
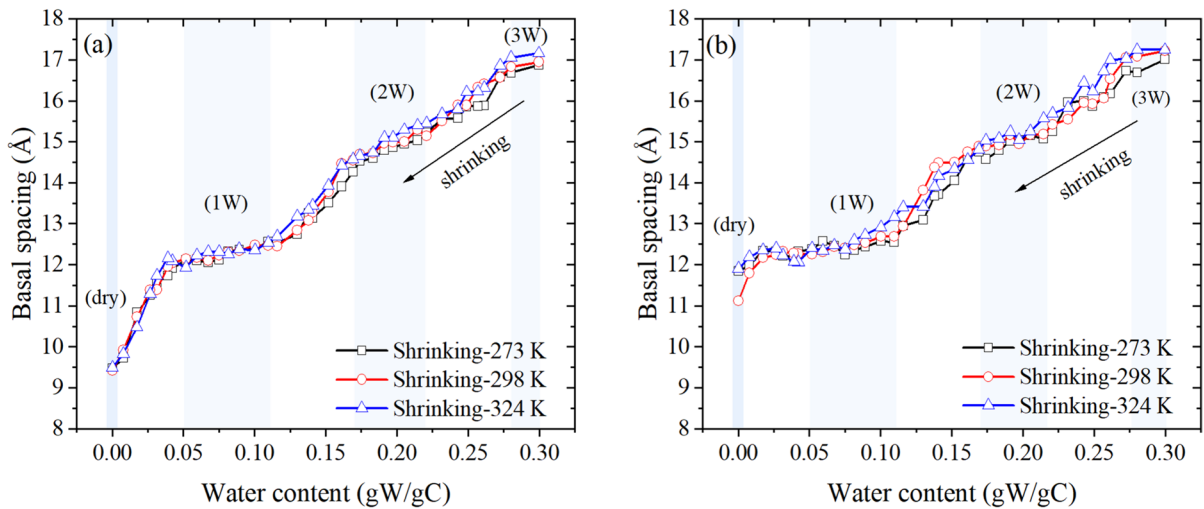
Fig. 5 The basal spacing of Na-MMT as a function of water content with various temperatures and water environments during the shrinkage: **a** fresh water; **b** salt water

spacing of 342 K is the largest. Moreover, at dry state, the MMT has higher basal spacing in salt water compared to fresh water, mainly due to the salt anions at the middle of the interlayer.

As shown in Fig. 6, the density profiles of interlayer ions in salt water simulations have peaks in the middle of the interlayer, which can be interpreted as a midplane formation of salt anions, whereas the interlayer ions peaks in fresh water simulations are close to clay surface oxygen.

In the following sections, the interaction energy between the components of Na-MMT (layer–layer, layer–cation, layer–water and water–cation) will be presented and the effect of the temperature and the water salinity on the interaction energy will be discussed. Interaction energy is the contribution of inter-component interactions to the total potential energy between these components. The positive interaction energy represents the repulsive interaction, while the negative interaction energy indicates the attractive interaction between the two atoms and/or molecules.

3.1 Effects of temperature on the interaction energy

In this section, we will discuss the interaction energy between the four components of Na-MMT during the shrinkage in fresh water at 273 K, 298 K and 324 K.

3.1.1 Interaction between layers (LL)

The interactions between clay layers are crucial for understanding the complex dynamics within the interlayer of Na-MMT. Figure 7 shows the interaction energies between two MMT layers as a function of the water layers in the interlayer at various temperatures: (a) 273 K, (b) 298 K and (c) 324 K. The Coulombic forces are repulsive due to the like charges of the layers, while the vdW interactions can be attractive at sufficient distances, providing some stabilization to the structure. It is found that the repulsive Coulombic interactions are close to zero with the large separation by three water layers (3W) between the MMT layers, reaching about 1.1 kcal/mol for 17 Å of layer spacing. However, the interactions rise slightly at two water layers (2W), with the water content in the interlayer falling to 0.20 gW/gC. At one water layer (1W), these interactions maintain increasing before jumping to the peak point (up to 330 kcal/mol) at dry state (0W). Similarly, the attractive van der Waals interactions grow as the distance between layers decreases due to the desorption of water. At three water layers, the van der Waals interactions are as small as around 0.2 kcal/mol, and reach an apex of around 110 kcal/mol at dry state. Such behavior was previously observed in a study of the swelling behavior of Na-MMT (Katti
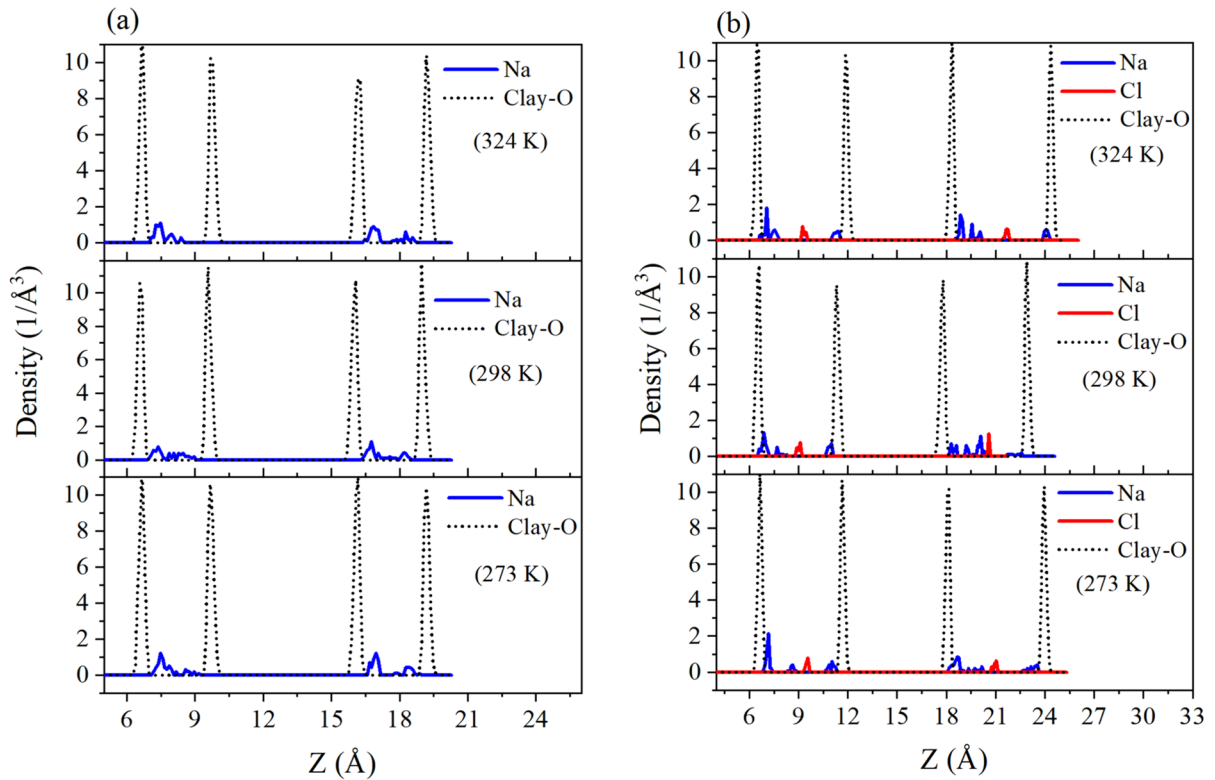
Fig. 6 Density profile of interlayer ions and clay surface oxygen (Clay-O) for Na-MMT at dry state, at 273 K, 298 K and 324 K: **a** fresh water; **b** salt water
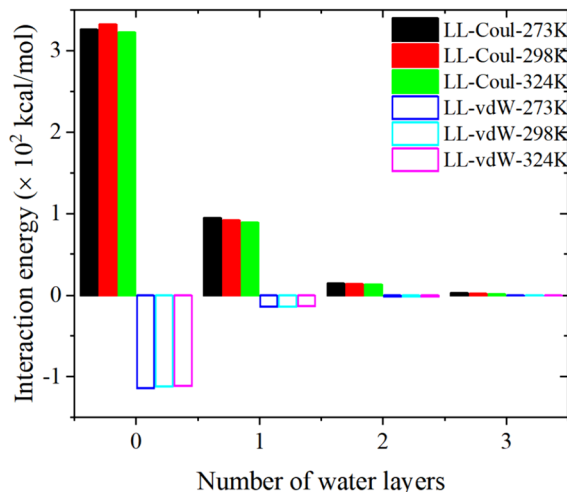

Fig. 7 The interaction energies between clay layers (LL): Coulombic (Coul) and van der Waals (vdW) interactions, with the change of interlayer water layers at 273 K, 298 K and 324 K

et al. 2008), but the van der Waals attractive interactions still are dominant at dry state, which differs from the observation in this study that the repulsive Coulombic interactions are dominant even at dry state. In general, both Coulombic and van der Waals interactions are almost the same with different temperatures, which means that the temperature effect on the LL interaction is negligible.

The overall controlling interactions between the atoms of the two adjacent clay layers are the repulsive Coulombic interactions and the attractive van der Waals interactions are not large enough to hold the layer together. This suggests that the interaction between clay layers has a slight impact on the MMT structure's stability, which is governed by the interaction of other interlayer components.
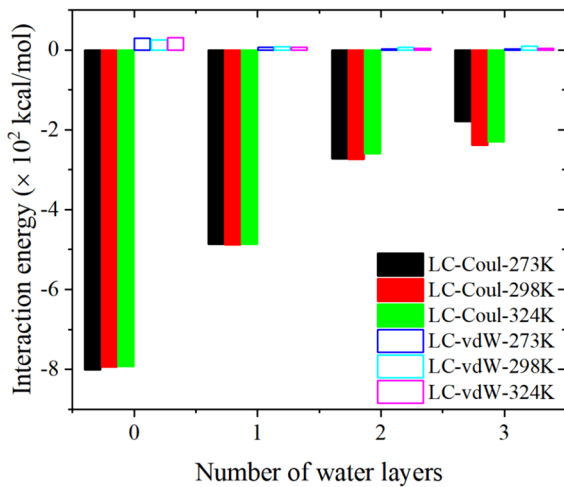
Fig. 8 The interaction energies between clay layers and interlayer cations (LC): Coulombic (Coul) and Van der Waals (vdW) interactions, with the change of interlayer water layers at 273 K, 298 K and 324 K

3.1.2 Interaction between layers and cations (LC)

The LC interactions are collected and shown in Fig. 8. Coulombic forces are attractive because of the opposite charges of the layers and cations, while the vdW interactions may appear repulsive at very short distances due to electron cloud repulsion. The layers–cations interaction energies increase significantly as the water content decreases because of the desorption of interlayer water molecules. At the beginning of the shrinkage, with three water layers, the van der Waals and Coulombic interactions are frail. It seems that, at three water layers, the interlayer cations interact greatly with the interlayer water molecular rather than with the clay layers, as indicated in Fig. 9. This may be because the cation tends to form an out-sphere complex and lends to the middle plan of the interlayer. Contrarily, at low interlayer water content (1W) and dry state (0W), the interlayer cations interact strongly with the layers because the cations tend to the clay mineral surface to form inner-sphere surface complexes. These results are in agreement with the previous study of the layers–Na interaction of Na-MMT (Pradhan 2015), in which the LC interactions increase as the water content in the interlayer decreases. In addition, it can be seen that the temperature effect on the interactions between layers–cations is obvious

just at higher hydrate state (3W) and the Coulombic interactions at 273 K are the smallest followed by 324 K and 298 K.

These results corroborate previous findings that the total interaction energies between clay layers and interlayer cations are attractive and predominantly determined by Coulombic interactions (Liu et al. 2021). Through the comparison between Figs. 7 and 8, the magnitude of attractive interactions between LC overcome the LL repulsive interactions, and thus, these attractive LC interaction energies are dominant to hold the MMT layers together, especially at dry state.

3.1.3 Interaction between interlayer water molecules and cations (WC)

Figure 9 plots the WC interaction energies during the shrinkage processes, as a function of water layers. With three layers of hydration, the interactions are attractive Coulombic and repulsive van der Waals interactions and the general interactions are primarily governed by Coulombic interactions. The attractive Coulombic interactions rise slightly at two water layers before disappearing at dry state. Furthermore, the strong Coulombic interactions at two water layers (2W) keep the water molecules nearby to the interlayer ions. This suggests that, at this hydration level, the interlayer cations are completely hydrated. Besides, at higher hydrate state (3W and 2W) the temperature effect is remarkable that the interactions decrease as temperature increases, but at low hydrate state (1W) the interactions dropped down at 273 K. A correlation could be drawn between the diffusion coefficient presented by Zhang et al. (2013) and the interaction energy of the interlayer cations and water molecules, in which the diffusion coefficient increases as interlayer water and temperature increase while the interaction energy decreases. Moreover, Teich-McGoldrick et al. (2015) noted that the stability of hydration shells around cations and the clay surface varies with temperature. The hydration shells are more stable at lower temperatures, leading to more consistent interaction energies.

According to the results of LC and WC in Figs. 8 and 9, it can be found that the interlayer cations interact much more greatly with water at high water content. As interlayer water desorption, these cations tend to be attracted strongly to the clay surface and dominant in binding the MMT layers together at the dry state.
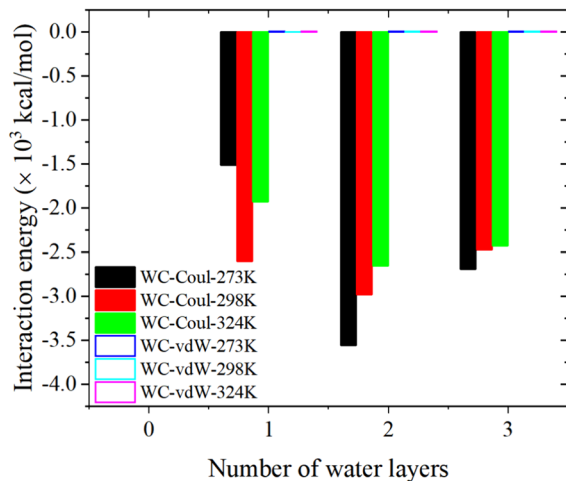
Fig. 9 The interaction energies between interlayer water and interlayer cations (WC): Coulombic (Coul) and Van der Waals (vdW) interactions, with the change of water layers at 273 K, 298 K and 324 K

3.1.4 Interaction between layers and interlayer water molecules (LW)

The LW interaction energies as a function of the water layers are plotted in Fig. 10. The interactions between clay layers and water molecules are attractive and derived by the Coulombic interactions. Note that the van der Waals interactions are negligible compared
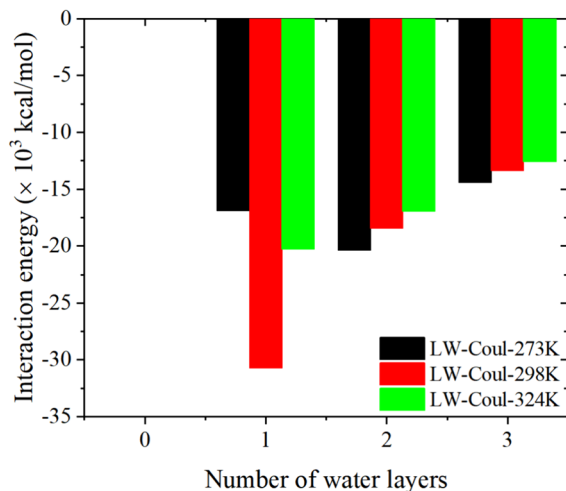
Fig. 10 The interaction energies between clay layers and interlayer water (LW): Coulombic (Coul) interactions, with the change of interlayer water layers at 273 K, 298 K and 324 K

to the Coulombic interactions and are not included in the results. The Coulombic interactions rise obviously with the desorption of the interlayer water, when transit from three to one water layers, then decreases to reach zero at the dry state. The hydration film of water molecules disappeared because of water molecule desorption, and the interaction in the dry state disappeared as well. Furthermore, it is clear that the interaction energy is also influenced by the temperature, which is higher at relatively low temperatures and decreases as temperature increases, with the exception in the case of 1W at 273 K where the interactions fell down similar to the interactions of WC at the same case.

In general, the effect of temperature on the interactions between Na-MMT components did not follow a consistent trend across different types of interactions. Specifically, LL and LC interactions exhibited varying responses to temperature changes, while WC and LW interactions generally decreased with increasing temperature. This variability can be attributed to the increased entropy resulting from thermal dispersion at higher temperatures. According to Smith et al. (2006), the swelling behavior and interaction energies in clays are influenced by temperature through entropy changes. At higher temperatures, the increased thermal motion of water molecules and ions leads to greater entropy, which disrupt the interactions among interlayer water molecules and ions (Whitley and Smith 2004).

Furthermore, the significant magnitude of attractive interactions between the clay layers and the associated water molecules means that the water molecules are tightly bound to the clay layers. Additionally, at hydrated state (1W, 2W and 3W), the substantial attractive interaction energy caused by LW interactions as well as WC far beyond compensates the weak attractive LL and LC interactions. Thus, the LW and WC interactions play a substantial role in the stability of hydrated clay at a hydrated state. However, they decrease with the increasing interlayer hydrated state, the interlayer separation, as well as the temperature.

3.2 Effect of salinity on the interaction energy

The interaction energy between the four components of Na-MMT and the effect of the salt water on these interactions will be discussed and compared to that in

fresh water at three temperatures, 273 K, 298 K and 324 K.

3.2.1 Interaction between layers (LL) in salt water

The LL interaction energies for salt and fresh water simulations are shown in Fig. 11. It is found that the interaction energy obtained from fresh water simulation is stronger than that from salt water simulation at various temperatures. These interactions are fairly similar at higher hydrate state (2W and 3W), but different at lower interlayer hydrate (1W) and dry state (0W). At one water layer, the main reason for the distinction between the interaction in salt and fresh water should be attributed to the salt anions attracted to the water molecules in the interlayer. Thus, the interactions contributed by the water to the clay layer are weaker than those in fresh water, and so are the interactions between the clay layers. At dry state, the attractive van der Waals and the repulsive Coulombic interactions are meager in salt water simulation due to the large d-spacing caused by the middle plan form of salt anions in the interlayer. In addition, at dry state, the interactions in fresh water almost remain the same at various temperatures compared to that in salt water, in which the Coulombic interactions are 100.4, 170 and 69.4 kcal/mol and the van der Waals interactions are -18, -37.3 and -11.8 kcal/mol for 273 K, 298 K 324 K, respectively. It is obvious that both the Coulombic and van der Waals interactions of layers are lower at 324 K, possibly because the interlayer ions diffuse faster and cause larger layer separation at higher temperatures as mentioned.

3.2.2 Interaction between layers and cations (LC) in salt water

Figure 12 shows the LC interaction energies for salt and fresh water simulations. At hydrated state (1W, 2W and 3W), the Coulombic interactions of salt water simulations are stronger than that in fresh water, but the opposite is true at dry state. This indicates that dry clay layers are less connected in saline environment when salt ions diffuse into the interlayer space, and are easier to rehydrate and swell again than that in the non-saline environment at the early stages of the swelling process. For van der Waals interactions, same phenomena of Coulombic interactions are observed, despite that the values are smaller compared to Coulombic interactions.

3.2.3 Interaction between interlayer water molecules and cations (WC) in salt water

The WC interaction energies for salt and fresh water simulations are shown in Fig. 13. The Coulombic interactions in salt water are slightly larger than that in fresh water under the same water layer.

All of this is due to hydration variations between interlayer cations and anions in the interlayer as well as the formation of the hydrogen bond between water and clay layers as can see from the hydrogen bond (HB) discussion in the following paragraphs. However, there is an exchangeable trend of the interaction energy between fresh and salt simulations at the same interlayer water layer, and this behavior is substantial for 1W at 298 K.
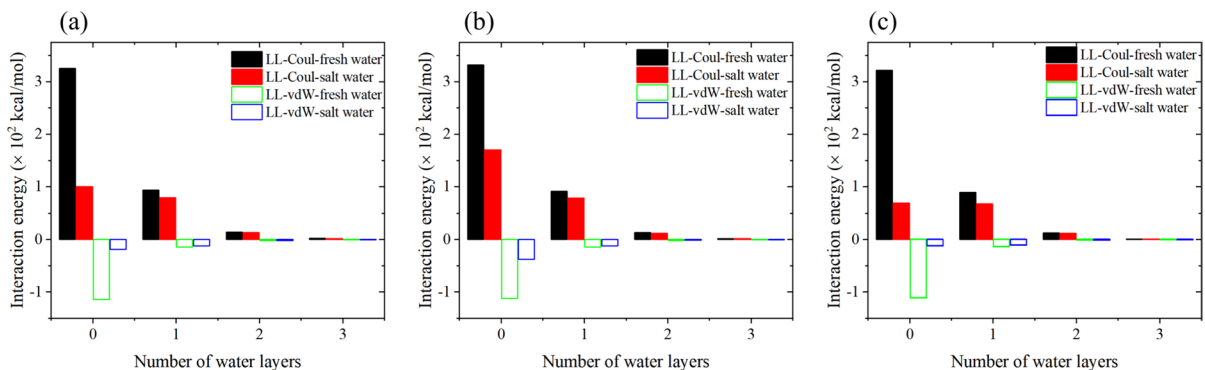

Fig. 11 The interaction energies between clay layers (LL), Coulombic (Coul) and Van der Waals (vdW) interactions, with the change of interlayer water layers for fresh and salt water simulation: **a** 273 K, **b** 298 K and **c** 342 K
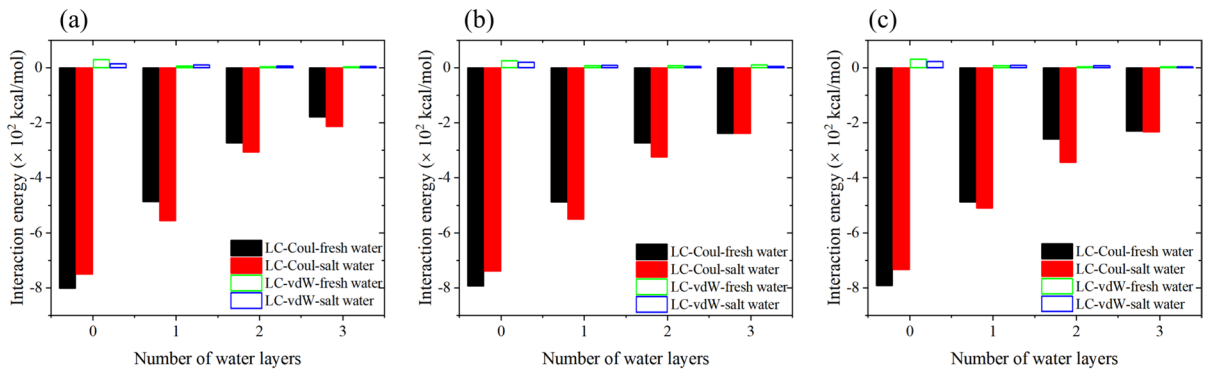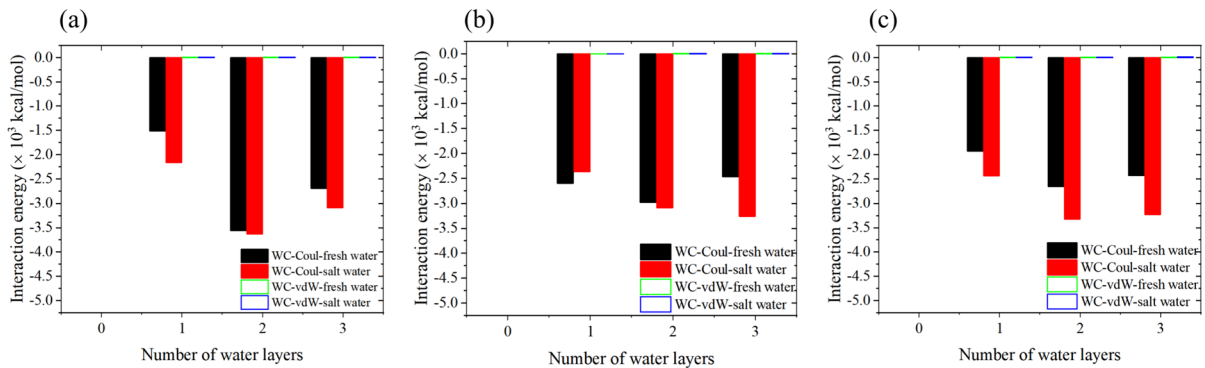
Fig. 12 The interaction energies between clay layers and interlayer cations (LC), Coulombic (Coul) and Van der Waals (vdW) interactions, with the change of interlayer water layers for fresh and salt water simulation: **a** 273 K, **b** 298 K and **c** 342 K

Fig. 13 The interaction energies between interlayer water and interlayer cations (WC), Coulombic (Coul) and van der Waals (vdW) interactions, with the change of interlayer water layers for fresh and salt water simulation: **a** 273 K, **b** 298 K and **c** 342 K

The interlayer water molecules in Na-MMT are connected by chains of hydrogen bonds that form between the interlayer water and clay surface as well as interlayer ions. The geometric standards for computing the water hydrogen bond included a cutoff distance of $r < 3.5$ Å for hydrogen-bonded pairs and an angle $< 30°$ between the O–H bond. In this study, the cutoff distance for hydrogen-bonded pairs was set to 2.4 Å, with a bond angle of 30° between H···O–O (Wei et al. 2021; Martí 1999). Figure 14 shows the number of hydrogen bonds and the average of hydrogen bonds per water molecule as a function of water content in both fresh and salt water simulations. It was found that the hydrogen bond number in salt water is higher than in fresh-water. Possible explanation is that in fresh water, hydrogen bonds form between water molecules and

also between water molecules and clay surface oxygen. At the same time, the interlayer Na^+ strongly attracts the water oxygen atoms, making water molecules tilt toward the orientation that prefers to donate hydrogen bonds. In salt water, however, the presence of salt anion (Cl^-) forms hydrogen bonds with hydrogen atoms of water. This additional source of hydrogen bonding increases the number of hydrogen bonds in salt water Na-MMT system. The formation of HB can vary based on specific conditions and ion concentrations. Svoboda et al. (2018) highlighted that the ion concentration stabilizes the clay structure more effectively than pure water, indicating that saline environments can enhance the stability of clay layers by increasing the hydrogen bond network. Conversely, Meng et al. (2022) found that salt ions affect the hydration layers on mineral
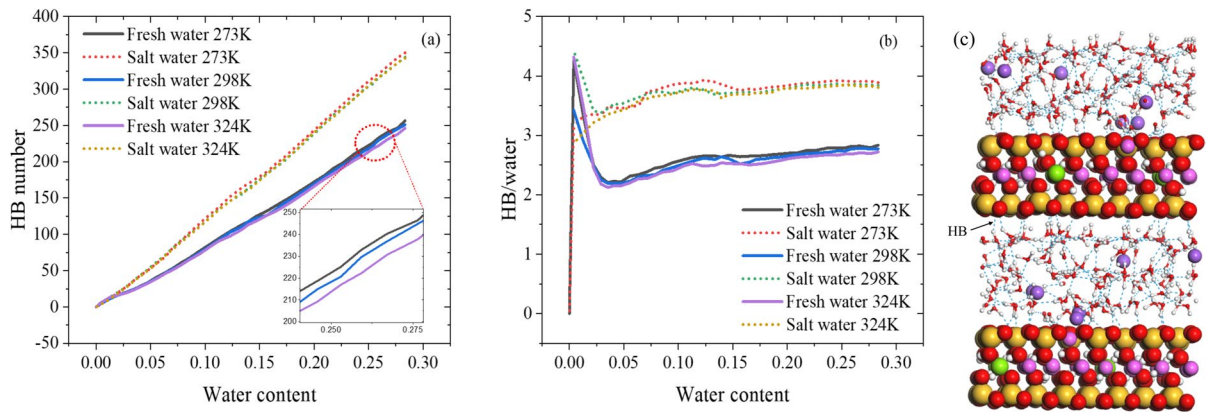
Fig. 14 The hydrogen bond between water molecules, and between water molecules and clay surface with the change of interlayer water content for fresh and salt water simulation at 273 K, 298 K and 324 K: **a** the number of hydrogen bond; **b** the average number of hydrogen bond per water molecular; **c** illustration of hydrogen bonds in MD simulation

surfaces, leading to a more disordered water structure and reduced hydrogen bonding. This indicates that in saline environments, the presence of Na^+ and Cl^- ions enhances the overall hydrogen bonding within the Na-MMT structure due to the formation of additional ion-water hydrogen bonds. However, at a local level, salt ions can disrupt the hydrogen bond network among water molecules, particularly affecting hydration layers and water structure density. These findings suggest that the interlayer water in salt water is more strongly connected, which may result in relatively weaker Na-MMT shrinkage in salt water compared to fresh water. Nevertheless, this effect can vary depending on the type of interlayer cation, such as Ca^{2+} or K^+, which K^+ is known to act as a swelling inhibitor and could alter the interaction dynamics and shrinkage behavior (Li et al. 2019; Malani and Ayappa 2009). Additionally, the number of hydrogen bonds decreases slightly at higher temperatures. This reduction is likely caused by the diminishing hydration shells around interlayer cations and salt anions and the weakened attractive forces exerted by the clay surface on water molecules at higher temperatures. This phenomenon explains the decrease in WC and LW interactions with increasing temperature.

The average number of hydrogen bonds shows that the fully hydrogen-bonded state is characterized by around 2.5 HBs per water in fresh water and about 3.5 HBs per water in salt water. At low hydrate state, in fresh water simulations, the average number of hydrogen bonds increased significantly as a result of the ability of water molecules to form more hydrogen bonds with the upper and bottom clay layer at relatively smaller basal spacing. Conversely, in salt water simulations, the average number of hydrogen bonds declined at low hydrate state, with the exaptation of 298 K case, due to the larger basal spacing. For salt water simulation at 298 K, the basal spacing is smaller; therefore, the formation of the hydrogen bonds at low hydrate state is similar to that in fresh water.

3.2.4 Interaction between layers and interlayer water molecules (LW) in salt water

The LW interaction energies for salt and fresh water simulations are shown in Fig. 15. There is an exchangeable trend of the interaction energy between fresh and salt simulations at the same water layer and temperature. The interaction energy of the fresh and salt water simulations is quite similar at three water layers (3W) at the same temperature and varies when interlayer water content decreases, especially at the lower interlayer water content (1W). All this fluctuation is related to the different hydration of the interlayer ions in both fresh and salt water.
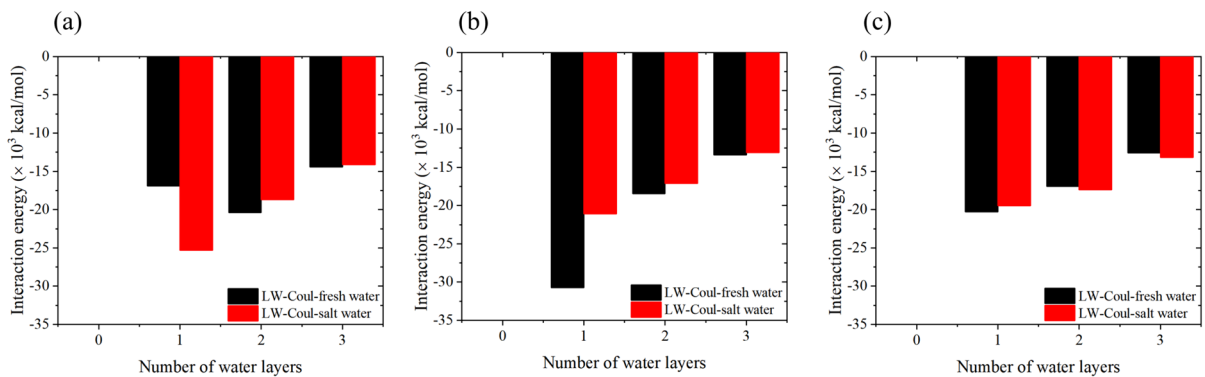
Fig. 15 The interaction energies between clay layers and interlayer water (LW), Coulombic (Coul) interactions, with the change of interlayer water layers for fresh and salt water simulation: **a** 273 K, **b** 298 K and **c** 342 K

4 Conclusions

In this study, molecular dynamics (MD) and Grand canonical Monte Carlo (GCMC) simulations were performed to quantitively determine the interaction energies between the MMT layers and the interlayer species and to investigate the shrinkage mechanism of Na-MMT. The interactions between MMT layers (LL), layer–cation (LC), layer–water (LW) and water–cation (WC) are presented and discussed. Several important conclusions can be drawn as follows:

1. The Coulombic interactions of MMT components are the major factor accounting for the stability of stacked layers of MMT. The interlayer shrinkage is determined by the extent of the interaction energy contributed by the interlayer cations dehydration.
2. At higher water content and basal spacing, the LW and WC interactions become more dominant. The stacked clay structure kept its stability at the start of the shrinkage (three water layers) in both salted and unsalted environments, mainly due to the attractive interaction between cations and water as well as between water and clay layers.
3. The interaction energy of LC appears to be the most important factor in keeping the stacked layers together and providing structural stability to the clay sheets in the dry state.
4. The interactions of LL and LC show fluctuating slightly with increasing temperature, while WC and LW interactions generally decrease with increasing temperature. This variability can be

attributed to the increased entropy resulting from thermal dispersion at higher temperatures.
5. Salt environment greatly increases the interaction energies of LC and WC at hydrated state; however, at dry state, the interaction energies of LL and LC are greater in fresh water, which is related to smaller basal spacing.

In summary, this study illustrates the variation of interaction energy in the Na-montmorillonite clay's interlayer during the desorption of the interlayer water and gives insight into shrinkage mechanisms which promotes further research into how clay components interact in various environments.

Author contributions W-QF: Conceptualization, Methodology, Investigation, Writing—Original Draft, Funding acquisition; KA-Z: Validation, Data Curation, Writing—Original Draft; Z-JC: Conceptualization, Investigation, Writing—Review and Editing.

Availability of data and materials Data and materials used in this study are available from the authors on reasonable request.

Declarations

Ethical approval No ethical approcal is needed.

Competing interests The authors have no competing interests as defined by Springer, or other interests that might be perceived to influence the results and/or discussion reported in this paper.

References

Acharya R, Pedarla A, Bheemasetti TV, Puppala AJ, Zhang N (2015) Shrinkage induced pressure measurement to address desiccation cracking in expansive soils. In: IFCEE 2015, pp 2122–2130

Ahmed HR, Abduljauwad SN (2017) Nano-level constitutive model for expansive clays. Geotechnique 67(3):187–207

Al-Zaoari K, Zheng YY, Wei PC, Zhang LL, Yin ZY (2022) Early stage of swelling process of dehydrated montmorillonite through molecular dynamics simulation. Mater Chem Phys 283:126015

Amarasinghe PM, Anandarajah A (2012) Behavior of swelling clays: a molecular dynamic study. In: GeoCongress 2012: state of the art and practice in geotechnical engineering, pp 2452–2461

Amarasinghe PM, Anandarajah A (2013) Molecular dynamic study of the swelling behavior of Na-montmorillonite. Environ Eng Geosci 19(2):173–183

Anandarajah A, Amarasinghe PM (2013) Discrete-element study of the swelling behaviour of Na-montmorillonite. Geotechnique 63(8):674–681

Anderson RL, Ratcliffe I, Greenwell HC, Williams PA, Cliffe S, Coveney PV (2010) Clay swelling—a challenge in the oilfield. Earth Sci Rev 98(3–4):201–216

Aoyama M, Joyce TM, Kawano T, Takatsuki Y (2002) Standard seawater comparison up to P129. Deep Sea Res Part I Oceanogr Res Pap 49(6):1103–1114

Berendsen HJ, Postma JP, van Gunsteren WF, Hermans J (1981) Interaction models for water in relation to protein hydration. In: Intermolecular forces: proceedings of the fourteenth Jerusalem symposium on quantum chemistry and biochemistry held in Jerusalem, Israel, April 13–16. Springer Netherlands, pp 331–342

Boek ES (2014) Molecular dynamics simulations of interlayer structure and mobility in hydrated Li-, Na-and K-montmorillonite clays. Mol Phys 112(9–10):1472–1483

Boek ES, Coveney PV, Skipper NT (1995) Monte Carlo molecular modeling studies of hydrated Li-, Na-, and K-smectites: understanding the role of potassium as a clay swelling inhibitor. J Am Chem Soc 117(50):12608–12617

Botan A, Rotenberg B, Marry V, Turq P, Noetinger B (2011) Hydrodynamics in clay nanopores. J Phys Chem C 115(32):16109–16115

Bowers GM, Singer JW, Bish DL, Kirkpatrick RJ (2011) Alkali metal and H_2O dynamics at the smectite/water interface. J Phys Chem C 115(47):23395–23407

Birgersson M, Karnland O (2009) Ion equilibrium between montmorillonite interlayer space and an external solution—consequences for diffusional transport. Geochim Cosmochim Acta 73(7):1908–1923

Camara M, Xu J, Wang X, Zhang J, Chen Z, Li X (2017) Molecular dynamics simulation of hydrated Na-montmorillonite with inorganic salts addition at high temperature and high pressure. Appl Clay Sci 146:206–215

Chang FRC, Skipper NT, Sposito G (1995) Computer simulation of interlayer molecular structure in sodium montmorillonite hydrates. Langmuir 11(7):2734–2741

Chen ZJ, Feng W, Li A, Al-Zaoari KYM, Yin JH (2023) Experimental and molecular dynamics studies on the consolidation of Hong Kong marine deposits under heating and vacuum preloading. Acta Geotech 18(5):2569–2583

Cygan RT, Liang JJ, Kalinichev AG (2004) Molecular models of hydroxide, oxyhydroxide, and clay phases and the development of a general force field. J Phys Chem B 108(4):1255–1266

Cygan RT, Greathouse JA, Kalinichev AG (2021) Advances in clayff molecular simulation of layered and nanoporous materials and their aqueous interfaces. J Phys Chem C 125(32):17573–17589

Du J, Zhou A, Shen SL, Lin X, Bu Y, Kodikara J (2022) Revealing crucial effects of temperature and salinization on swelling behavior of montmorillonite. Chem Eng J 429:132263

Dai W-J, Chen Y-G, Ye W-M, Wang Q, Wu D-B (2023) Thermal and saline effects on the swelling deformation of montmorillonite: a molecular dynamics study. Bull Eng Geol Environ 83(1):11

Ewis D, Ba-Abbad MM, Benamor A, El-Naas MH (2022) Adsorption of organic water pollutants by clays and clay minerals composites: a comprehensive review. Appl Clay Sci 229:106686

Fu MH, Zhang ZZ, Low PF (1990) Changes in the properties of a montmorillonite-water system during the adsorption and desorption of water: hysteresis. Clays Clay Miner 38:485–492

Ghazanfari S, Alesadi A, Liao Y, Zhang Y, Xia W (2023) Molecular insights into the temperature and pressure dependence of mechanical behavior and

dynamics of Na-montmorillonite clay. Nanoscale Adv 5(20):5449–5459

Katti DR, Thapa KB, Katti KS (2018) The role of fluid polarity in the swelling of sodium-montmorillonite clay: a molecular dynamics and Fourier transform infrared spectroscopy study. J Rock Mech Geotech Eng 10(6):1133–1144

He Y, Ye WM, Chen YG, Zhang KN, Wu DY (2020) Effects of NaCl solution on the swelling and shrinkage behavior of compacted bentonite under one-dimensional conditions. Bull Eng Geol Env 79(1):399–410

Henok Hailemariam FW (2021) Effects of drying and shrinkage on the mechanical performance of unsaturated fine/medium-grained soils used as heat storage media. MATEC Web Conf 337:01022

Humphrey W, Dalke A, Schulten K (1996) VMD: visual molecular dynamics. J Mol Graph 14(1):33–38

Li A, Feng WQ, Chen ZJ, Mailk N, Yin JH, Zhou C (2024) Investigation and analysis of the macro- and micro-responses of bentonite-sand mixtures to temperature. Geomech Energy Envir 38:100565

Li X, Li Q, Yang S, Yang G (2019) Swelling of clay minerals: dual characteristics of K(+) ions and exploration of critical influencing factors. Phys Chem Chem Phys 21(4):1963–1971

Li Y-C, Wei S-J, Xu N, He Y (2020) Internal forces within the layered structure of Na-montmorillonite hydrates: molecular dynamics simulation. J Phys Chem C 124(46):25557–25567. https://doi.org/10.1021/acs.jpcc.0c07597

Liu L, Zhang C, Jiang W, Li X, Dai Y, Jia H (2021) Understanding the sorption behaviors of heavy metal ions in the interlayer and nanopore of montmorillonite: a molecular dynamics study. J Hazard Mater 416:125976

Liu ZR, Ye WM, Cui YJ, Zhu HH, Wang Q (2022) Temperature effects on water retention behaviour and structural evolution of GMZ bentonite pellet mixtures. Appl Clay Sci 222:106492

Loganathan N, Yazaydin AO, Bowers GM, Kalinichev AG, Kirkpatrick RJ (2016) Structure, energetics, and dynamics of Cs+ and H_2O in hectorite: molecular dynamics simulations with an unconstrained substrate surface. J Phys Chem C 120(19):10298–10310

Katti D, Katti K, Schmidt S, Ghosh P, Matar M, Chatterjee S, Amarasinghe P (2008) A Multiscale computational and experimental investigation of swelling clay behavior: bridging scales using steered molecular dynamics, modified discrete element method and experiments. In: The 12th international conference of international association for computer methods and advances in geomechanics (IACMAG)

Marry V, Turq P, Cartailler T, Levesque D (2002) Microscopic simulation of structure and dynamics of water and counterions in a monohydrated montmorillonite. J Chem Phys 117(7):3454–3463

Martí J (1999) Analysis of the hydrogen bonding and vibrational spectra of supercritical model water by molecular dynamics simulations. J Chem Phys 110(14):6876–6886

Malani A, Ayappa KG (2009) Adsorption isotherms of water on mica: redistribution and film growth. J Phys Chem B 113(4):1058–1067

Meng J, Li C, Yan S, Zhang S, Zhang H, Wang G, Yang X (2022) Atomic-level insights into the mechanism of

saline-regulated montmorillonite (001)-salt droplet interface wetting: a molecular dynamics study. Appl Clay Sci 224:106513

Norrish K (1954) The swelling of montmorillonite. Discuss Faraday Soc 18:120–134

Pradhan SM, Katti KS, Katti DR (2015) Evolution of molecular interactions in the interlayer of Na-montmorillonite swelling clay with increasing hydration. Int J Geomech 15(5):04014073

Plimpton S (1995) Fast parallel algorithms for short-range molecular dynamics. J Comput Phys 117(1):1–19

Smith DE, Wang Y, Chaturvedi A, Whitley HD (2006) Molecular simulations of the pressure, temperature, and chemical potential dependencies of clay swelling. J Phys Chem B 110(40):20046–20054

Song Z, Zhang Z, Lu Y, Du X (2024) Shrinkage behavior of compacted bentonite considering physicochemical effects. Sci Total Environ 906:167547

Svoboda M, Moučka F, Lísal M (2018) Saturated aqueous NaCl solution and pure water in Na-montmorillonite clay at thermodynamic conditions of hydraulic fracturing: thermodynamics, structure and diffusion from molecular simulations. J Mol Liq 271:490–500

Tajeddine L, Gailhanou H, Blanc P, Lassin A, Gaboreau S, Vieillard P (2015) Hydration–dehydration behavior and thermodynamics of MX-80 montmorillonite studied using thermal analysis. Thermochim Acta 604:83–93

Teich-McGoldrick SL, Greathouse JA, Jové-Colón CF, Cygan RT (2015) Swelling properties of montmorillonite and beidellite clay minerals from molecular simulation: comparison of temperature, interlayer cation, and charge location effects. J Phys Chem C 119(36):20880–20891

Villar MV, Gómez-Espina R, Gutiérrez-Nebot L (2012) Basal spacings of smectite in compacted bentonite. Appl Clay Sci 65:95–105

Vydelingum S, Levitz P, Michot LJ, Bizien T, Rabu P, Ersen O et al (2023) Clay platelet orientation inside self-standing beidellite clay films: Effect of silica nanospheres and link with macroscopic mechanical resistance. Appl Clay Sci 231:106740

Wang G, Wei X (2015) Modeling swelling–shrinkage behavior of compacted expansive soils during wetting–drying cycles. Can Geotech J 52(6):783–794

Wei PC, Zhang LL, Zheng YY, Diao QF, Zhuang DY, Yin ZY (2021) Nanoscale friction characteristics of hydrated montmorillonites using molecular dynamics. Appl Clay Sci 210:106155

Wei P, Zheng YY, Xiong Y, Zhou S, Al-Zaoari K, Zaoui A (2022) Effect of water content and structural anisotropy on tensile mechanical properties of montmorillonite using molecular dynamics. Appl Clay Sci 228:106622

Whitley HD, Smith DE (2004) Free energy, energy, and entropy of swelling in Cs-, Na-, and Sr-montmorillonite clays. J Chem Phys 120(11):5387–5395

Young DA, Smith DE (2000) Simulations of clay mineral swelling and hydration: dependence upon interlayer ion size and charge. J Phys Chem B 104(39):9163–9170

Yotsuji K, Tachi Y, Sakuma H, Kawamura K (2021) Effect of interlayer cations on montmorillonite swelling: comparison

between molecular dynamic simulations and experiments. Appl Clay Sci 204:106034

Zhang X, Yi H, Zhao Y, Min F, Song S (2016) Study on the differences of Na- and Ca-montmorillonites in crystalline swelling regime through molecular dynamics simulation. Adv Powder Technol 27(2):779–785

Zheng Y, Zaoui A (2011) How water and counterions diffuse into the hydrated montmorillonite. Solid State Ionics 203(1):80–85

Zheng Y, Zaoui A (2013) Temperature effects on the diffusion of water and monovalent counterions in the hydrated montmorillonite. Physica A 392(23):5994–6001

Zheng Y, Zaoui A, Shahrour I (2010) Evolution of the interlayer space of hydrated montmorillonite as a function of temperature. Am Miner 95(10):1493–1499

Zheng Y, Zaoui A, Shahrour I (2011) A theoretical study of swelling and shrinking of hydrated Wyoming montmorillonite. Appl Clay Sci 51(1–2):177–181

Zhang L, Lu X, Liu X, Zhou J, Zhou H (2014) Hydration and mobility of interlayer ions of (Nax, Cay)-montmorillonite: a molecular dynamics study. J Phys Chem C 118(51):29811–29821